Cell Communication and Signaling

BRIEF REPORT Open Access

Knockout of PAK1 and PAK4 supresses tumour growth associated with vasculogenic mimicry inhibition through EphA2–VE-cadherin–MCAM pathway

Arian Ansardamavandi[1], Chelsea Dumesny[1], Sarah Ellis[2,3], Ching-Seng Ang[4], Mehrdad Nikfarjam[1,5] and Hong He[1*]

Abstract

Pancreatic ductal adenocarcinoma (PDA) remains largely refractory to anti-angiogenic strategies, and non-endothelial perfusion mechanisms such as vasculogenic mimicry (VM, endothelial-like channels formed by tumour cells) may sustain tumour progression. Here, we examined whether the combined knockout of p21-activated kinase 1 and 4 (PAK1&4) affects vascular mimicry (VM) programmes in pancreatic cancer. KPC wild-type or PAK1&4 knockout cells were injected subcutaneously into immunodeficient mice. Knockout of PAK1& 4 suppressed tumour growth, associated with VM inhibition, but not endothelial angiogenesis. Knockout of PAK1& 4 reduced tumour expression of VM markers EphA2, VE-cadherin and MCAM, and decreased EphA2$^+$VE-cadherin$^+$ and EphA2$^+$MCAM$^+$, CD31$^+$VE-cadherin$^+$ and CD31$^+$MCAM$^+$ cells. In vitro, PAK1 knockout and PAK1& 4 knockout suppressed VM-like tube formation and migration, whereas PAK4 knockout enhanced tube formation. Global proteomics linked PAK1 knockout to downregulation of EPH–Ephrin signalling and reduced EphA2–MCAM–RhoA abundance, while PAK4 knockout enriched blood-vessel morphogenesis molecules. These findings identify a PAK-dependent VM programme and suggest that dual PAK targeting inhibits tumour growth by VM inhibition.

Keywords Pancreatic ductal adenocarcinoma, p21-activated kinases, Vasculogenic mimicry, EphA2, VE-cadherin, Hypoxia

Introduction

Pancreatic ductal adenocarcinoma (PDA) remains a lethal malignancy with limited therapeutic options and a tumour microenvironment characterised by profound stromal remodelling and abnormal microcirculation [1]. Clinical targeting of vascular endothelial growth factor (VEGF) signalling has shown limited benefit in advanced pancreatic cancer, highlighting that endothelial sprouting angiogenesis alone is unlikely to explain or therapeutically control tumour perfusion in this disease [2]. Beyond endothelial angiogenesis, tumours can adopt alternative vascularisation strategies, including vasculogenic mimicry (VM), the ability of aggressive cancer cells to form

*Correspondence:
Hong He
hong.he@unimelb.edu.au
[1]Department of Surgery, Austin Precinct, The University of Melbourne, 145 Studley Rd, Melbourne, VIC 3084, Australia
[2]Olivia Newton-John Cancer Research Institute, Melbourne, VIC 3086, Australia
[3]School of Cancer Medicine, La Trobe University, Melbourne, VIC 3000, Australia
[4]Mass Spectrometry and Proteomics Facility, Bio21 Molecular Science and Biotechnology Institute, University of Melbourne, Parkville, VIC 3010, Australia
[5]Department of Hepatopancreatic-Biliary Surgery, Austin Health, 145 Studley Rd, Melbourne, VIC 3084, Australia

matrix-rich channel-like networks that can connect with endothelial vessels and support tumour growth [3]. VM is detected histologically as a Periodic acid–Schiff (PAS)-positive/CD31-negative structure and has been associated with tumour aggressiveness and therapy resistance [4].

Mechanistically, VM relies on tumour cell plasticity and an endothelial-like transcriptional/phenotypic programme. VEGF contributes to VM by activating VEGFR-dependent pathways that enhance tumour-cell motility, matrix remodelling and endothelial-like gene programmes, thereby facilitating $PAS^+/CD31^-$ channel formation [5]. Vascular endothelial cadherin (VE-cadherin) is required for VM network formation, and functional cooperation between VE-cadherin and Ephrin receptor A2 (EphA2) has been implicated in the establishment and maintenance of VM structure [6]. In addition, melanoma cell adhesion molecule (MCAM)/CD146 is frequently linked to migratory, vascular-interactive phenotypes and has been connected to VM and vascular mimicry-associated cell states [7, 8].

P21-activated kinases (PAKs) are central effectors downstream of Rho-family GTPases, regulating cytoskeletal dynamics, migration, and vascular interactions in cancer and endothelium [9]. While PAK signalling has been implicated in tumour vasculature regulation, whether combined PAK1 and PAK4 activity supports VM programme in PDA remains unclear [10, 11]. Here, using a pancreatic cancer model with single or combined knockout (KO) of PAK1 and PAK4, we showed that PAK1&4 knockout reduced tumour growth associated with VM suppression via downregulation of EphA2–VE-cadherin–MCAM pathway.

Results

Knockout of PAK1 and PAK4 restrained tumour growth and suppressed vasculogenic mimicry while increasing hypoxia

KPC wild-type (WT) and KPC PAK1&4KO cells were injected subcutaneously into SCID mice to evaluate tumour progression. PAK1&4KO suppressed tumour growth by reducing tumour volume (Fig. 1a, b). The tumour weight, however, was not significantly reduced by PAK1&4KO (Fig. S1a). Histopathological assessment showed a significant reduction in necrotic area in PAK1&4KO tumours (Fig. S1b), indicating altered tumour composition, which could contribute to the insignificant reduction of tumour weight by PAK1&4KO.

In addition to reduced tumour size, PAK1&4KO tumours exhibited a visibly paler appearance, which was confirmed by quantitative greyscale analysis showing a higher background-normalised mean grey value relative to WT (Fig. 1b, c). Although our previous study reported no significant change in endothelial angiogenesis in PAK1&4KO tumours [11], the paler macroscopic appearance of PAK1&4KO tumours suggested altered intratumoural vascular function and/or perfusion (Fig. 1b, c).

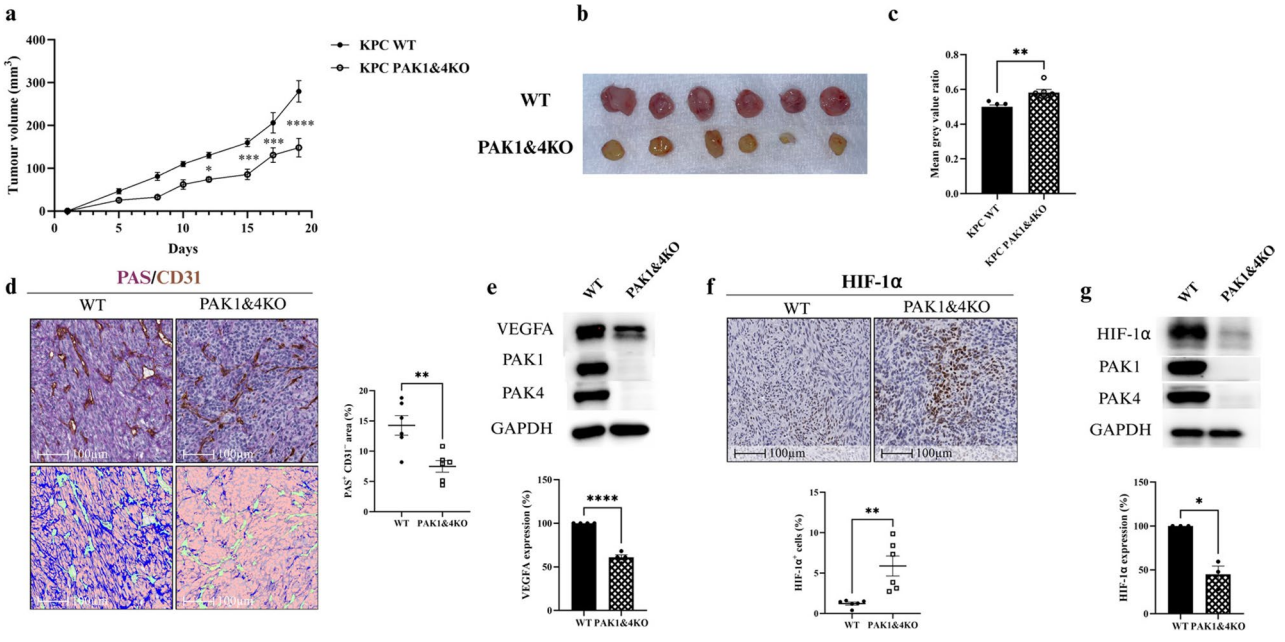

Fig. 1 PAK1&4KO restrained tumour growth, reduced VM and increased tumour hypoxia. (**a**) Tumour volume growth curves (SCID; $n=6$ WT, $n=6$ PAK1&4KO). (**b**) Tumour images. (**c**) Mean grey value with background-normalised using a local background ROI (tumour mean/background mean). (**d**) PAS/CD31 double staining and VM quantification ($PAS^+/CD31^-$ structures). The blue colour indicates the $PAS^+/CD31^-$ overlay of the PAS analysis by HALO. (**e**) VEGFA levels in PAK1&4KO cells. (**f**) HIF-1α expression in tumour tissues. (**g**) HIF-1α levels in PAK1&4KO cells. WT, wild type; KO, knockout; ns, not significant. $^*P<0.05$, $^{**}P<0.01$, $^{***}P<0.001$, $^{****}P<0.0001$

We therefore examined tumour-cell–mediated VM identified by $PAS^+/CD31^-$ structure in tumour tissues. VM was reduced in PAK1&4KO tumours (Fig. 1d). In parallel, VEGFA expression was decreased in PAK1&4KO cells compared with WT cells (Fig. 1e), consistent with VM suppression in PAK1&4KO tumours (Fig. 1d).

The reduced VM was associated with increased hypoxia in vivo, demonstrated by increased HIF-1α-positive cells in PAK1&4KO tumours (Fig. 1f). In contrast, HIF-1α expression was decreased in PAK1&4KO cells (Fig. 1g). These findings indicated that the reduction of VM by PAK1&4KO decreased intratumoral perfusion, increasing hypoxia in PAK1&4KO tumours. We also attempted to establish double-knockout tumours in C57BL/6 mice; however, tumours regressed completely within 10 days (Fig. S2), precluding subsequent VM analyses. This rapid regression in immunocompetent hosts suggests robust immune activation and infiltration, consistent with our prior reports of enhanced immune responses following PAK1 and 4 knockout in C57BL/6 models [10, 12]. Therefore, double-knockout analyses were performed only in immunocompromised mice. PAS/CD31 analysis of tumours derived from single knockout cell lines showed that VM was not significantly altered by PAK1KO or PAK4KO alone in either SCID xenografts or BL6 tumours (Fig. S2). Together, these data suggested that VM may be maintained following single-kinase knockout in vivo, whereas robust suppression of VM is achieved when both PAK1 and PAK4 are knocked out simultaneously.

PAK1 and PAK4 knockout inhibited VM associated with suppression of EphA2, VE-cadherin, and MCAM

Given the reported association of VM with upregulation of EphA2, VE-cadherin and MCAM [7, 13], we assessed these markers in tumour tissues. Immunohistochemistry (IHC) demonstrated reduced EphA2, VE-cadherin and MCAM expression in PAK1&4KO tumours compared

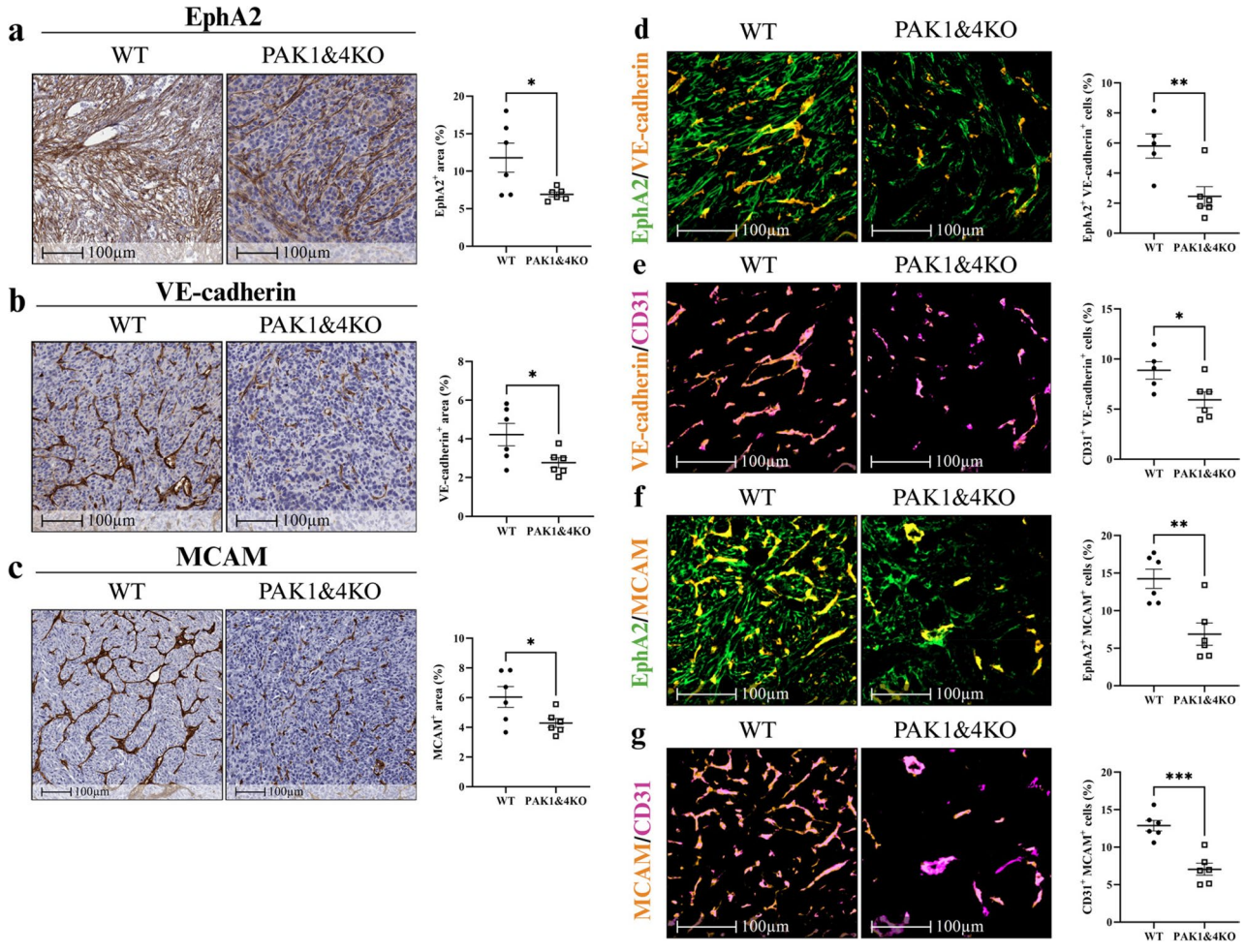

Fig. 2 PAK1&4KO reduced VM-associated markers of EphA2, VE-cadherin and MCAM. (**a**–**c**) Representative IHC and quantification of EphA2, VE-cadherin and MCAM. (**d**–**g**) Multiplex IHC and quantification of $EphA2^+VE\text{-}cadherin^+$ cells, $CD31^+VE\text{-}cadherin^+$ cells, $EphA2^+MCAM^+$ cells and $CD31^+MCAM^+$ cells. WT, wild type; KO, knockout. $^*P < 0.05$, $^{**}P < 0.01$, $^{***}P < 0.001$

with WT, quantified as a decrease in marker-positive area (Fig. 2a–c, S4b-c, S5b), consistent with the reduced VM phenotype (Fig. 1d).

To define the cellular context of these changes, multiplex immunohistochemistry was used to examine co-expression patterns consistent with VM-like and vascular-interactive phenotypes. EphA2⁺VE-cadherin⁺ cells were decreased in PAK1&4KO tumours (Fig. 2d, S4a), demonstrating reduced tumour cells that simultaneously express the VM-associated receptor EphA2 and the endothelial junction protein VE-cadherin, consistent with suppression of an endothelial-like (VM-competent) tumour cell phenotype. Similarly, EphA2⁺MCAM⁺ cells were reduced (Fig. 2f, S5a), supporting suppression of VM-competent subsets marked by simultaneous EphA2 and MCAM expressions.

In parallel, CD31⁺VE-cadherin⁺ and CD31⁺MCAM⁺ cells were decreased (Fig. 2e and g, S4a, S5a), indicating reduced VE-cadherin and MCAM expression within vascular-associated compartments, thus reduced endothelial junction in vessels [14, 15]. In contrast, the proportion of CD31⁺ cells remained unchanged (Fig. S4d). These findings indicate that PAK1&4KO suppressed VM-associated endothelial-like programme significantly rather than the overall endothelial angiogenesis (CD31⁺ vasculature).

PAK knockout differentially regulates in vitro tube formation and cancer cell migration

To validate the VM phenotype in vitro, we assessed the tube formation capability of WT, PAK1KO, PAK4KO, and PAK1&4KO cancer cells. Compared to WT, PAK1KO cells formed significantly fewer tube-like structures, indicating impaired VM-like network formation, while PAK4KO cells showed increased tube formation (Fig. 3a). Notably, PAK1&4KO significantly reduced tube formation compared to WT (Fig. 3b), aligning with the reduced VM detected in tumours (Fig. 1d) and decreased VM-associated marker expression in vivo (Fig. 2).

Because VM competence is closely linked to tumour cell motility [6], we evaluated migration using scratch assays. PAK1KO and PAK1&4KO cells significantly reduced migration rate and delayed wound healing (%) at 24 h compared with WT (Fig. 3c), consistent with impaired motility.

Proteomic profiling identified Eph/Ephrin signalling as a PAK1-dependent programme and revealed a pro-vascular signature in PAK4KO cells

To define the molecular pathways underlying the divergent VM phenotypes across PAK KO, we performed unbiased global proteomics comparing PAK1KO,

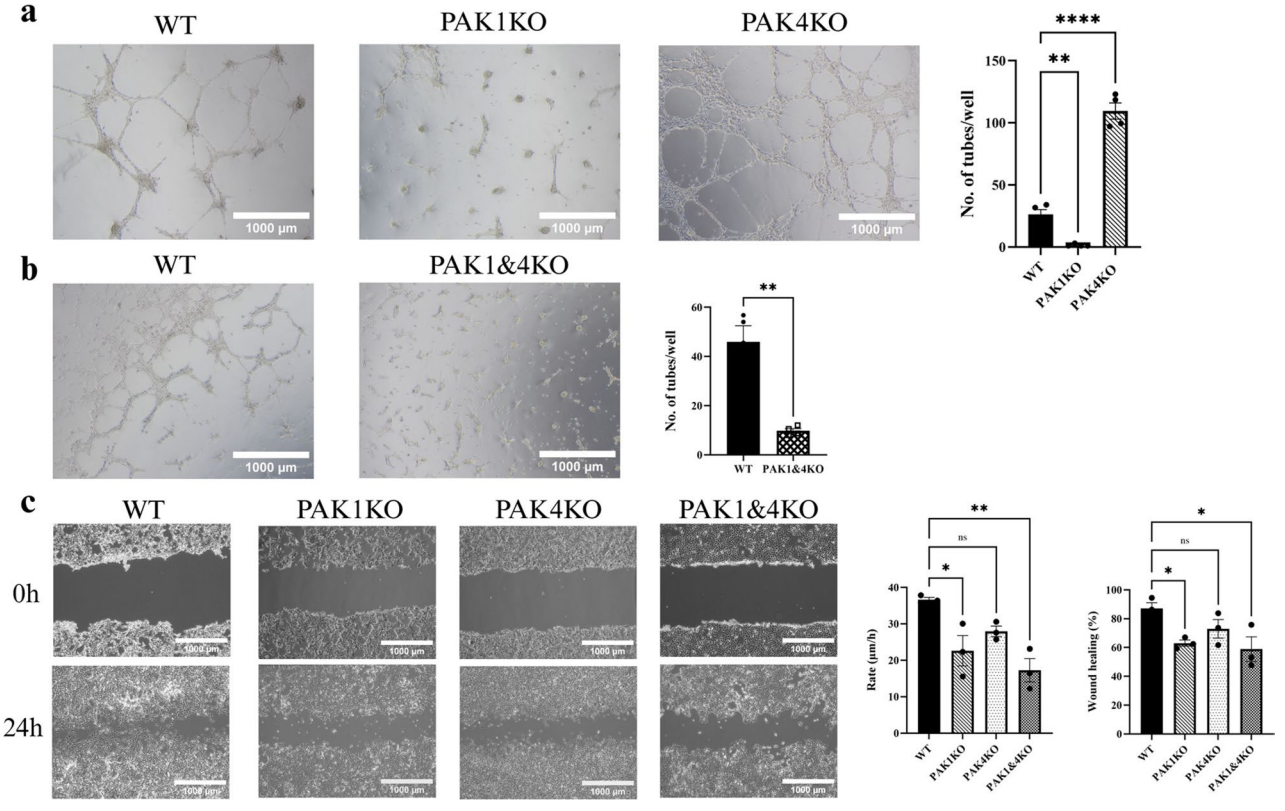

Fig. 3 PAK knockout differentially regulated tube formation and cancer cell migration in vitro. (**a**) Tube formation assay (WT, PAK1KO, PAK4KO) with quantification of tube structures. (**b**) Tube formation assay (WT vs. PAK1&4KO) with quantification. (**c**) Scratch assay images (0, 24 h) with migration rate and wound healing (%) calculated for 24 h. WT, wild type; KO, knockout; ns, not significant. *$P < 0.05$, **$P < 0.01$, ****$P < 0.0001$

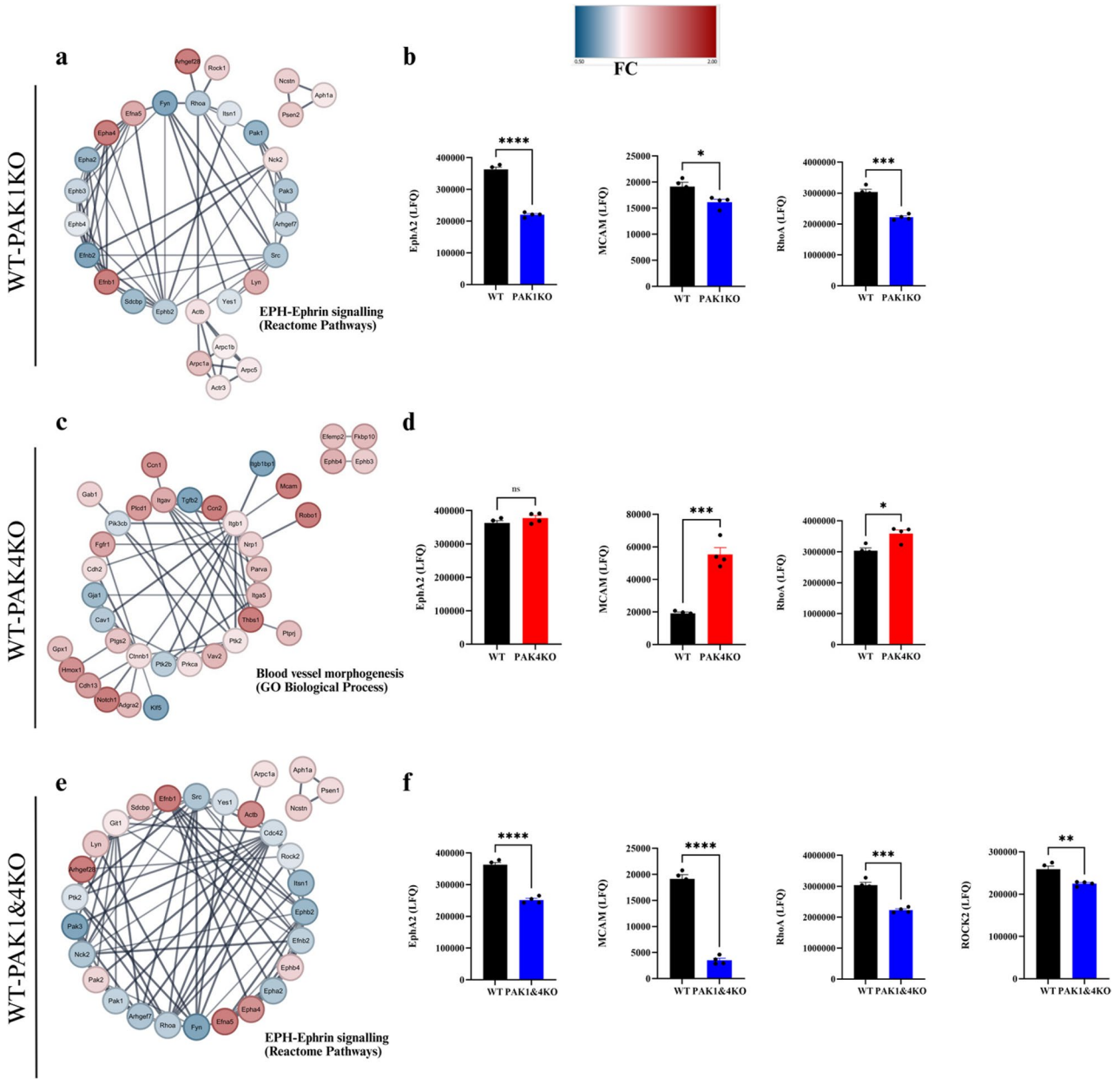

Fig. 4 Proteomics identified PAK1-dependent suppression of EPH–Ephrin signalling and genotype-specific VM effector regulation. (**a**, **e**) PPI networks highlighting EPH–Ephrin signalling downregulation (Reactome) in PAK1KO (a) and PAK1&4KO (e). (**c**) PPI network highlighting blood vessel morphogenesis enrichment (GO Biological Process) in PAK4KO. (**b**, **d**, **f**) VM-related protein abundance changes (EphA2, MCAM, RhoA ± ROCK2). LFQ, label-free quantification; FC, fold change; ns, not significant. *$P < 0.05$, **$P < 0.01$, ***$P < 0.001$, ****$P < 0.0001$

PAK4KO and PAK1&4KO cells with WT controls. Protein–protein interaction (PPI) network analysis of significantly altered proteins showed a coherent downregulation of the EPH–Ephrin signalling pathway (Reactome) in PAK1KO and PAK1&4KO cells (Fig. 4a, e), identifying Eph/Ephrin signalling in a PAK1-linked network, disrupted by PAK1KO. An enrichment of proteins associated with blood vessel morphogenesis (GO Biological Process) was shown in PAK4KO cells (Fig. 4c), consistent with a pro-vascular/VM-supportive signature in PAK4KO cells.

Inspection of VM-relevant effectors supported these pathway-level findings. PAK1KO cells exhibited significant reductions in EphA2, MCAM and RhoA (Fig. 4b), consistent with reduced tube formation and migration (Fig. 3a, c). PAK1&4KO cells showed broader suppression of VM-associated proteins, including significant reductions in EphA2, MCAM, Ras homolog family member A (RhoA) and Rho-associated coiled-coil containing

protein kinase 2 (ROCK2) (Fig. 4f), consistent with reduced VM in tumours (Fig. 1d). Conversely, PAK4KO cells showed an opposing pattern, with significant increases in MCAM and RhoA (Fig. 4d), providing a molecular basis for enhanced tube formation in PAK4KO cells (Fig. 3a).

Discussion

Our previous study established distinct vascular functions of PAK1 and PAK4 in pancreatic tumours: PAK1 inhibition suppressed tumour growth and promoted vascular normalisation (reduced angiogenesis and increased vessel stability), whereas PAK4 knockout enhanced gemcitabine efficacy with variable effects on tumour regression [11]. Building on this framework, the present study showed that PAK1&4KO inhibited VM, providing a complementary mechanism of vascular reprogramming beyond alterations in endothelial angiogenesis. PAK1&4KO reduced tumour growth by decreasing tumour volume and produced a paler macroscopic phenotype (Fig. 1a–c). Given the significantly reduced necrotic area in PAK1&4KO tumours (Fig. S1b), the tumour weight may not accurately reflect viable tumour growth because tumour weight can be excessively influenced by differences in necrosis, oedema/haemorrhage, and non-malignant stromal/ECM content; therefore, tumour volume was prioritised as the primary growth factor in this study [16].

PAK1&4KO decreased $PAS^+/CD31^-$ VM structures but did not affect endothelial abundance as overall CD31 expression remained unchanged (Fig. S4d), indicating that PAK1&4KO predominantly restricted tumour-cell vascular plasticity rather than depleting endothelial vessels.

The inhibition of VM by PAK1&4KO was associated with downregulation of EphA2, VE-cadherin, and MCAM. EphA2 and VE-cadherin are established regulators of VM network formation and tumour cell endothelial-like behaviour, with prior work demonstrating that VE-cadherin modulates EphA2 activity in the context of VM [17]. MCAM/CD146 has been implicated in vascular-interactive phenotypes and VM-associated states across tumour types [18]. The reductions in $EphA2^+$VE-$cadherin^+$ and $EphA2^+MCAM^+$ tumour cell subsets, alongside decreased CD31-associated VE-cadherin/MCAM signals, suggest that PAK1&4KO limits both VM-competent tumour cell populations and their vascular interface.

Increased HIF-1α expression in PAK1&4KO tumour, while decreased HIF-1α levels in PAK1&4KO cells, suggested that increased hypoxia in tumour is likely microenvironment-driven (Fig. 1f-g). VM is proposed to act as an adaptive perfusion strategy under stress, and hypoxia is a recognised inducer of VM-associated programmes in multiple tumour settings, including pancreatic cancer [4]. In this context, our findings indicated that reduced VM as an alternative perfusion route may increase hypoxia signalling, even when $CD31^+$ endothelial content is preserved.

Our data indicated a PAK-isoform–dependent regulation of VM. In vitro, PAK1KO reduced tube formation and migration (Fig. 3a, c), implying decreased VM frameworks, emphasising tumour-cell plasticity as a prerequisite for network formation [19]. The reduction of EPH–Ephrin signalling (Fig. 4a, e) and downregulation of core VM effectors—EphA2, MCAM and RhoA, by PAK1KO and PAK1&4KO from the proteomic study (Fig. 4b, f) showed clear mechanism involved in the impaired migration and tube formation (Fig. 3). In contrast, PAK4KO increased tube formation (Fig. 3a) and displayed an enriched blood vessel morphogenesis signature (Fig. 4c), with increased abundance of MCAM and RhoA (Fig. 4d), indicating that PAK4KO shifted tumour cells toward a VM-permissive state. Notably, VM was not significantly altered in vivo by PAK1KO or PAK4KO (Fig. S3). PAK1KO reduced endothelial angiogenesis [10, 11]. This suggests that VM may be maintained independently of endothelial vessel abundance in vivo, that microenvironment-driven plasticity preserved tumour perfusion routes despite reduced angiogenesis. Together, these findings support a model in which robust VM suppression requires simultaneous knockout of PAK1 and PAK4.

PAK family kinases are well-recognised downstream effectors of Rac and Cdc42 that coordinate cytoskeletal remodelling, cell–cell adhesion, and vascular patterning through regulation of actin dynamics and Rho GTPase signalling [20, 21]. Both EphA2 signalling and VE-cadherin-mediated junctional organisation are highly dependent on these cytoskeletal processes, and EphA2 is a central regulator of VM, functioning through VE-cadherin and MCAM-dependent pathways [7, 22–24]. Consistent with these established mechanisms, our proteomic and in vivo analyses demonstrate that combined PAK1/PAK4 knockout is associated with suppression of Eph–Ephrin signalling components and reduced expression of EphA2, VE-cadherin, and MCAM in tumours.

RhoA/ROCK signalling represents an additional point of convergence linking PAK activity to VM. PAK1 has been reported to negatively regulate RhoA signalling through phosphorylation of upstream regulators, whereas PAK4 can modulate actin organisation and adhesion in a context-dependent manner [25–27]. This provides a mechanistic explanation for our observation that PAK4 knockout alone enhances tube-like structure formation and is associated with increased MCAM and RhoA pathway activity, while concurrent knockout of both PAK1 and PAK4 decreases RhoA/ROCK expression and suppresses VM formation in vivo. These

findings suggest that functional redundancy and cross-regulation between PAK1 and PAK4 are required to maintain the cytoskeletal plasticity and adhesive interactions necessary for VM. Together, these data support a model in which PAK1/PAK4 coordinate with EphA2–VE-cadherin–MCAM signalling through Rho GTPase-dependent cytoskeletal control, thereby enabling VM formation, while dual kinase knockout disrupts this network and suppresses VM.

Anti-VEGF approaches have not improved survival in PDA clinical trials, underscoring the need to target non-endothelial vascularisation mechanisms [2]. In this study, concurrent knockout of PAK1 and PAK4 suppressed VM without substantially altering $CD31^+$ endothelial abundance, indicating a non-endothelial signalling dependency that may be therapeutically relevant. Importantly, our study defines a tumour-cell–intrinsic genetic dependency of VM on concurrent loss of PAK1 and PAK4, rather than evaluating pharmacological PAK inhibition. Given that non-selective Group I PAK inhibition can be limited by on-target toxicity associated with PAK2 engagement [28, 29], any translational extension of these findings would most plausibly rely on isoform-selective approaches that minimise PAK2 inhibition. Notably, highly selective PAK1 chemical probes such as NVS-PAK1-1 have been developed with substantially weaker activity against PAK2 than against PAK1, enabling interrogation of PAK1 biology with reduced PAK2 engagement [30]. In parallel, PAK4-targeting compounds have shown anti-tumour activity in preclinical studies [31, 32]. Together, these observations support a hypothesis-generating framework in which selective PAK1 inhibition combined with PAK4 targeting could be explored to disrupt VM-associated signalling, pending rigorous optimisation of selectivity, target engagement, and safety.

Methods

Cell culture

Murine pancreatic cancer KPC lines (WT, PAK1KO, PAK4KO, PAK1&4KO) were generated as described previously [33] and maintained in Dulbecco's modified Eagle's medium (DMEM) + 5% foetal bovine serum (FBS) (Thermo Fisher Scientific, Melbourne, Australia) at 37 °C, 5% CO_2.

Animal studies

All procedures were approved by the Austin Health Animal Ethics Committee (A2022-05797; A2023-05849). Male SCID or C57BL/6 (BL6) mice (7 weeks old) received subcutaneous injections into the flank (0.5–1 × 10^6 cells in 100 µL per injection) and were monitored for 3 weeks. Tumour volume (mm^3) was calculated as $V = 0.5 \times L \times W^2$. At the endpoint, tumours were excised and weighed. PAK1&4KO tumours did not establish in BL6 mice [12]; therefore, double-knockout tumour analyses were confined to SCID mice.

To compare macroscopic tumour colour differences, endpoint photographs were converted to 8-bit greyscale in ImageJ. Each tumour was segmented to generate a whole-tumour region of interest (ROI) by selecting the external tumour boundary using the Wand (Tracing) tool with visual verification to exclude background. Mean grey value was measured within the tumour ROI. For background normalisation, a standardised local background ROI was placed on a clean area adjacent to each tumour (avoiding shadows, glare, and tumour edges) to measure background mean grey value. Tumour lightness was expressed as the mean grey value ratio (tumour/background), calculated as tumour mean grey value divided by background mean grey value.

IHC and PAS/CD31 vasculogenic mimicry

Formalin-fixed, paraffin-embedded tumours were sectioned (5 µm) using a Leica RM2245 microtome (Leica Biosystems, Nussloch, Germany). Antigen retrieval was performed in 10 mM Tris–EDTA (pH 9.0) at 99 °C for 30 min (Table S1). DAB-based IHC was performed using peroxidase blocking and HRP-polymer detection reagents (Agilent Technologies, Glostrup, Denmark) with primary antibodies listed in Table S2. Whole-slide images were acquired on an Aperio AT2 scanner (Leica Biosystems). For quantitative analysis, necrotic regions were manually excluded, and marker-positive area was quantified in HALO v4.1 (Indica Labs, Albuquerque, NM, USA) using fixed thresholds across all samples. For vasculogenic mimicry (VM) assessment, sections were first stained for CD31 by IHC and subsequently stained with a periodic acid–Schiff (PAS) kit (ab150680; Abcam, Cambridge, UK). VM structures were defined and quantified as $PAS^+/CD31^-$ regions in HALO v4.1.

Immunoblotting

Cells were lysed in 2× loading buffer (Table S1), resolved by 10% SDS–PAGE, transferred to nitrocellulose, and probed for HIF-1α, PAK1, PAK4, and GAPDH (Table S3). Signals were detected with HRP goat anti-rabbit IgG (Bio-Rad, Hercules, CA, USA) and ECL Select™ (Cytiva, Amersham, UK) and quantified in ImageJ with GAPDH normalisation.

Multiplex Immunohistochemistry (mIHC)

Sequential TSA-based staining was performed with one primary antibody per round, followed by HRP secondary and tyramide–Alexa Fluor deposition, with repeat antigen retrieval between rounds. Staining order/dyes were CD31 (AF647), VE-cadherin or MCAM (AF555), and EphA2 (AF488). Slides were counterstained with Spectral DAPI (Akoya Biosciences, Marlborough, MA, USA),

mounted with VECTASHIELD (Vector Laboratories, Burlingame, CA, USA), scanned on a Zeiss Axioscan 7 (Carl Zeiss AG, Oberkochen, Germany), and quantified in HALO v3.0.1 (Indica Labs) using constant thresholds.

Tube formation

Geltrex™ Basement Membrane Matrix (A1413202, Thermo Fisher Scientific) was thawed overnight at 4 °C and handled on ice. Pre-chilled 24-well plates were coated with 0.1 mL Geltrex per well and incubated at 37 °C for 30 min to allow polymerisation. WT, PAK1KO, PAK4KO and PAK1&4KO cells were resuspended in serum-free DMEM at 2×10^5 cells/mL, and 0.25 mL ($\sim 5 \times 10^4$ cells) was seeded onto each coated well. After 14–20 h incubation at 37 °C in 5% CO_2, tube-like network structures were imaged using an inverted microscope at 4× magnification, and the number of tubes per well was quantified manually by an observer blinded to group allocation. Each condition was analysed in four technical replicates.

Wound healing assay

Monolayers (~ 80% confluence) in 6-well plates were scratched with a 200 µL tip, washed with PBS, and imaged at 0, 24, and 48 h (4×; Leica Microsystems, Mannheim, Germany). Migration rate and wound healing (%) were calculated for 0–24 h as described [34] (triplicate).

Proteomics

Global proteomics of KPC WT, PAK1KO, PAK4KO, and PAK1&4KO cells was performed as previously described [11]. Briefly, cells were lysed in RIPA supplemented with protease/phosphatase inhibitors (Roche, Mannheim, Germany), and proteins were processed for liquid chromatography/mass spectrometry (LC–MS) using data-independent acquisition (DIA) (Table S1). Quantification and statistics were conducted in Perseus v2.1.3.0 using four biological replicates per group, with proteins retained if ≥ 3 valid values per group; differential abundance was assessed by two-sample Student's t-test with permutation-based false discovery rate (FDR) control (S_0 = 0.1; FDR < 0.05), and volcano plots were generated. STRING/Cytoscape network and enrichment analyses were performed as reported [11].

Statistical analysis

Data are presented as mean ± standard error of the mean (SEM). Comparisons between two groups were performed using an unpaired, two-tailed Student's t-test. For ≥ 3 groups, one-way ANOVA with Dunnett's multiple comparisons test was used. For analyses involving two independent variables, two-way ANOVA (including interaction) with Sidak's multiple comparisons test was applied. Statistical significance was defined as $P < 0.05$. Analyses were performed using GraphPad Prism v10.6.0 (GraphPad Software, San Diego, CA, USA).

Supplementary Information

The online version contains supplementary material available at https://doi.org/10.1186/s12964-026-02778-3.

Supplementary Material 1.

Acknowledgements

A.A. is supported by the postgraduate scholarship from the University of Melbourne and a top-up scholarship from Jreissati Pancreatic Centre, Epworth HealthCare. The Henry Baldwin Cancer Research Trust Fund supports HH.

Institutional Review Board Statement

The mouse study protocol was approved by the Austin Health Animal Ethics Committee (project numbers: A2022-05797 and A2023-05849).

Authors' contributions

Conceptualization, A.A., M.N. and H.H.; methodology, A.A., C.D., S.E., C.S.A., and H.H.; software, A.A., C.D., S.E., and C.S.A.; validation, C.D., and H.H.; formal analysis, A.A., C.D., and H.H.; investigation, A.A., C.D., L.D., Y.M., and H.H.; data curation, A.A., C.D., M.N., and H.H.; writing—original draft preparation, A.A., and H.H.; writ-ing—review and editing, A.A., C.D., S.E., C.S.A., M.N., and H.H.; visualization, A.A., C.D., and H.H.; supervision, M.N., and H.H.; project administration, M.N., and H.H.; funding acquisition, M.N., and H.H.; All authors have read and agreed to the published version of the manuscript.

Funding

This research was funded by the Austin Medical Research Foundation, grant numbers 2025-HH and 2024-MN and Pancare Foundation. This is an invited paper with the APC waived.

Data availability

The data will be available from the corresponding author on request.

Declarations

Ethics approval and consent to participate

Not applicable.

Competing interests

The authors declare no competing interests.

Received: 20 January 2026 / Accepted: 27 February 2026
Published online: 13 March 2026

References

1. Ansardamavandi A, Nikfarjam M, He H. PAK in Pancreatic Cancer-Associated Vasculature: Implications for Therapeutic Response. Cells. 2023;12(23):2692. https://doi.org/10.3390/cells12232692.
2. Kindler HL, Niedzwiecki D, Hollis D, Sutherland S, Schrag D, Hurwitz H, Innocenti F, Mulcahy MF, O'Reilly E, Wozniak TF, Picus J, Bhargava P, Mayer RJ, Schilsky RL, Goldberg RM. Gemcitabine plus bevacizumab compared with gemcitabine plus placebo in patients with advanced pancreatic cancer: phase III trial of the Cancer and Leukemia Group B (CALGB 80303). J Clin Oncol. 2010;28(22):3617–22. https://doi.org/10.1200/jco.2010.28.1386.
3. Hendrix MJ, Seftor EA, Seftor RE, Chao JT, Chien DS, Chu YW. Tumor cell vascular mimicry: Novel targeting opportunity in melanoma. Pharmacol Ther. 2016;159:83–92. https://doi.org/10.1016/j.pharmthera.2016.01.006.
4. Yang J, Zhu D-M, Zhou X-G, Yin N, Zhang Y, Zhang Z-X, Li D-C, Zhou J. HIF-2α promotes the formation of vasculogenic mimicry in pancreatic cancer by regulating the binding of Twist1 to the VE-cadherin promoter. Oncotarget. 2017;8(29):47801. https://doi.org/10.18632/oncotarget.17999.
5. Wang JY, Sun T, Zhao XL, Zhang SW, Zhang DF, Gu Q, Wang XH, Zhao N, Qie S, Sun BC. Functional significance of VEGF-a in human ovarian carcinoma: role

in vasculogenic mimicry. Cancer Biol Ther. 2008;7(5):758–66. https://doi.org/10.4161/cbt.7.5.5765.
6. Zhang J, Qiao L, Liang N, Xie J, Luo H, Deng G, Zhang J. Vasculogenic mimicry and tumor metastasis. J buon. 2016;21(3):533–41.
7. Zinovkin DA, Wang H, Yu Z, Zhang Q, Zhang Y, Wei S, Zhou T, Zhang Q, Zhang J, Nadyrov EA, Farooq A, Lyzikova Y, Vejalkin IV, Slepokurova II, Pranjol MZI. The vasculogenic mimicry, CD146(+) and CD105(+) microvessel density in the prognosis of endometrioid endometrial adenocarcinoma: a single-centre immunohistochemical study. Biomarkers. 2024;29(7):459–65. https://doi.org/10.1080/1354750x.2024.2415078.
8. Du X, Zhang Q, Wang S, Chen X, Wang Y. MCAM is associated with metastasis and poor prognosis in osteosarcoma by modulating tumor cell migration. J Clin Lab Anal. 2022;36(2):e24214. https://doi.org/10.1002/jcla.24214.
9. Radu M, Semenova G, Kosoff R, Chernoff J. PAK signalling during the development and progression of cancer. Nat Rev Cancer. 2014;14(1):13–25.
10. Ansardamavandi A, Dumesny C, Ma Y, Dong L, Ellis S, Ang C-S, Nikfarjam M, He H. P-21 Kinase 1 or 4 Knockout Stimulated Anti-Tumour Immunity Against Pancreatic Cancer by Enhancing Vascular Normalisation. Int J Mol Sci. 2025;26(17):8357. https://doi.org/10.3390/ijms26178357.
11. Ansardamavandi A, Dumesny C, Ma Y, Dong L, Ellis S, Ang C-S, Nikfarjam M, He H. The Effects of PAK-Regulated Tumour Vasculature on Gemcitabine Response of Pancreatic Cancer. Cancers. 2025;17(21). https://doi.org/10.3390/cancers17213434.
12. Ma Y, Dumesny C, Dong L, Ang C-S, Asadi K, Zhan Y, Nikfarjam M, He H. Inhibition of P21-activated kinases 1 and 4 synergistically suppresses the growth of pancreatic cancer by stimulating anti-tumour immunity. Cell Communication Signal. 2024;22(1):287. https://doi.org/10.1186/s12964-024-01670-2.
13. Fernández-Cortés M, Delgado-Bellido D, Oliver FJ. Vasculogenic Mimicry: Become an Endothelial Cell But Not So Much. Front Oncol. 2019;9:803. https://doi.org/10.3389/fonc.2019.00803.
14. Bardin N, Anfosso F, Massé JM, Cramer E, Sabatier F, Le Bivic A, Sampol J, Dignat-George F. Identification of CD146 as a component of the endothelial junction involved in the control of cell-cell cohesion. Blood. 2001;98(13):3677–84. https://doi.org/10.1182/blood.v98.13.3677.
15. Dejana E, Orsenigo F, Lampugnani MG. The role of adherens junctions and VE-cadherin in the control of vascular permeability. J Cell Sci. 2008;121(13):2115–22. https://doi.org/10.1242/jcs.017897.
16. Schuh JC. Trials, tribulations, and trends in tumor modeling in mice. Toxicol Pathol 32 Suppl. 2004;153–66. https://doi.org/10.1080/01926230490424770.
17. Hess AR, Seftor EA, Gruman LM, Kinch MS, Seftor RE, Hendrix MJ. VE-cadherin regulates EphA2 in aggressive melanoma cells through a novel signaling pathway: implications for vasculogenic mimicry. Cancer Biol Ther. 2006;5(2):228–33. https://doi.org/10.4161/cbt.5.2.2510.
18. Zhang R, Chen X, Chen S, Tang J, Chen F, Lin Y, Reinach PS, Yan X, Tu L, Duan H, Qu J, Hou Q. Inhibition of CD146 lessens uveal melanoma progression through reducing angiogenesis and vasculogenic mimicry. Cell Oncol (Dordr). 2022;45(4):557–72. https://doi.org/10.1007/s13402-022-00682-9.
19. Kirschmann DA, Seftor EA, Hardy KM, Seftor RE, Hendrix MJ. Molecular pathways: vasculogenic mimicry in tumor cells: diagnostic and therapeutic implications. Clin Cancer Res. 2012;18(10):2726–32. https://doi.org/10.1158/1078-0432.Ccr-11-3237.
20. Bokoch GM. Biology of the p21-activated kinases. Annu Rev Biochem. 2003;72:743–81. https://doi.org/10.1146/annurev.biochem.72.121801.161742.
21. Arias-Romero LE, Chernoff J. A tale of two Paks. Biol Cell. 2008;100(2):97–108. https://doi.org/10.1042/bc20070109.
22. Maniotis AJ, Folberg R, Hess A, Seftor EA, Gardner LM, Pe'er J, Trent JM, Meltzer PS, Hendrix MJ. Vascular channel formation by human melanoma cells in vivo and in vitro: vasculogenic mimicry. Am J Pathol. 1999;155(3):739–52. https://doi.org/10.1016/s0002-9440(10)65173-5.
23. Wang H, Lin H, Pan J, Mo C, Zhang F, Huang B, Wang Z, Chen X, Zhuang J, Wang D, Qiu S. Vasculogenic Mimicry in Prostate Cancer: The Roles of EphA2 and PI3K. J Cancer. 2016;7(9):1114–24. https://doi.org/10.7150/jca.14120.
24. Delgado-Bellido D, Serrano-Saenz S, Fernández-Cortés M, Oliver FJ. Vasculogenic mimicry signaling revisited: focus on non-vascular VE-cadherin. Mol Cancer. 2017;16(1):65. https://doi.org/10.1186/s12943-017-0631-x.
25. Alberts AS, Qin H, Carr HS, Frost JA. PAK1 negatively regulates the activity of the Rho exchange factor NET1. J Biol Chem. 2005;280(13):12152–61. https://doi.org/10.1074/jbc.M405073200.
26. Wells CM, Whale AD, Parsons M, Masters JR, Jones GE. PAK4: a pluripotent kinase that regulates prostate cancer cell adhesion. J Cell Sci. 2010;123(Pt 10):1663–73. https://doi.org/10.1242/jcs.055707.
27. Wells CM, Abo A, Ridley AJ. PAK4 is activated via PI3K in HGF-stimulated epithelial cells. J Cell Sci. 2002;115(Pt 20):3947–56. https://doi.org/10.1242/jcs.00080.
28. Rudolph J, Murray LJ, Ndubaku CO, O'Brien T, Blackwood E, Wang W, Aliagas I, Gazzard L, Crawford JJ, Drobnick J, Lee W, Zhao X, Hoeflich KP, Favor DA, Dong P, Zhang H, Heise CE, Oh A, Ong CC, La H, Chakravarty P, Chan C, Jakubiak D, Epler J, Ramaswamy S, Vega R, Cain G, Diaz D, Zhong Y. Chemically Diverse Group I p21-Activated Kinase (PAK) Inhibitors Impart Acute Cardiovascular Toxicity with a Narrow Therapeutic Window. J Med Chem. 2016;59(11):5520–41. https://doi.org/10.1021/acs.jmedchem.6b00638.
29. Binder P, Wang S, Radu M, Zin M, Collins L, Khan S, Li Y, Sekeres K, Humphreys N, Swanton E, Reid A, Pu F, Oceandy D, Guan K, Hille SS, Frey N, Müller OJ, Cartwright EJ, Chernoff J, Wang X, Liu W. Pak2 as a Novel Therapeutic Target for Cardioprotective Endoplasmic Reticulum Stress Response. Circ Res. 2019;124(5):696–711. https://doi.org/10.1161/circresaha.118.312829.
30. Chow HY, Karchugina S, Groendyke BJ, Toenjes S, Hatcher J, Donovan KA, Fischer ES, Abalakov G, Faezov B, Dunbrack R, Gray NS, Chernoff J. Development and Utility of a PAK1-Selective Degrader. J Med Chem. 2022;65(23):15627–41. https://doi.org/10.1021/acs.jmedchem.2c00756.
31. Murray BW, Guo C, Piraino J, Westwick JK, Zhang C, Lamerdin J, Dagostino E, Knighton D, Loi CM, Zager M, Kraynov E, Popoff I, Christensen JG, Martinez R, Kephart SE, Marakovits J, Karlicek S, Bergqvist S, Smeal T. Small-molecule p21-activated kinase inhibitor PF-3758309 is a potent inhibitor of oncogenic signaling and tumor growth. Proc Natl Acad Sci U S A. 2010;107(20):9446–51. https://doi.org/10.1073/pnas.0911863107.
32. He H, Dumesny C, Ang CS, Dong L, Ma Y, Zeng J, Nikfarjam M. A novel PAK4 inhibitor suppresses pancreatic cancer growth and enhances the inhibitory effect of gemcitabine. Transl Oncol. 2022;16:101329. https://doi.org/10.1016/j.tranon.2021.101329.
33. Wang K, Zhan Y, Huynh N, Dumesny C, Wang X, Asadi K, Herrmann D, Timpson P, Yang Y, Walsh K, Baldwin GS, Nikfarjam M, He H. Inhibition of PAK1 suppresses pancreatic cancer by stimulation of anti-tumour immunity through down-regulation of PD-L1. Cancer Lett. 2020;472:8–18. https://doi.org/10.1016/j.canlet.2019.12.020.
34. Suarez-Arnedo A, Torres Figueroa F, Clavijo C, Arbeláez P, Cruz JC, Muñoz-Camargo C. An image J plugin for the high throughput image analysis of in vitro scratch wound healing assays. PLoS ONE. 2020;15(7):e0232565. https://doi.org/10.1371/journal.pone.0232565.

Publisher's note